Available online at www.sciencedirect.com
SCIENCE DIRECT®
Journal of Solid State Chemistry 177 (2004) 709–713
JOURNAL OF SOLID STATE CHEMISTRY
http://elsevier.com/locate/jssc

Syntheses, structure, and magnetic properties of several $LnYbQ_3$ chalcogenides, $Q = S$, Se

Kwasi Mitchell, Rebecca C. Somers, Fu Qiang Huang, and James A. Ibers*

Department of Chemistry, Northwestern University, 2145 Sheridan Rd., Evanston, IL 60208-3113, USA

Received 3 June 2003; received in revised form 14 August 2003; accepted 11 September 2003

Abstract

The six $LnYbQ_3$ compounds β-$LaYbS_3$, $LaYbSe_3$, $CeYbSe_3$, $PrYbSe_3$, $NdYbSe_3$, and $SmYbSe_3$ have been synthesized from high-temperature solid-state reactions of the constituent elements at 1223 K. The compounds are isostructural to $UFeS_3$ and crystallize in the space group *Cmcm* of the orthorhombic system with four formula units in a cell. Cell constants (Å) at 153 K are: β-$LaYbS_3$, 3.9238(8), 12.632(3), 9.514(2); $LaYbSe_3$, 4.0616(8), 13.094(3), 9.932(2); $CeYbSe_3$, 4.0234(5), 13.065(2), 9.885(1); $PrYbSe_3$, 4.0152(5), 13.053(2), 9.868(1); $NdYbSe_3$, 4.0015(6), 13.047(2), 9.859(1); $SmYbSe_3$, 3.9780(9), 13.040(3), 9.860(2). The structure is composed of layers of YbQ_6 (Q = S or Se) octahedra that alternate with layers of LnQ_8 bicapped trigonal prisms along the *b*-axis. Because there are no Q–Q bonds in the structure the formal oxidation states of Ln/Yb/Q are 3+/3+/2−. Magnetic susceptibility measurements indicate that $CeYbSe_3$ and $SmYbSe_3$ are Curie–Weiss paramagnets over the temperature range 5–300 K.
© 2003 Elsevier Inc. All rights reserved.

Keywords: Synthesis; Crystal structure; Solid-state compound; Rare-earth element; Chalcogenide; Magnetic properties

1. Introduction

The $LnLn'O_3$ oxides, where Ln = La–Nd and Ln' = Ho–Lu, Y, have been the focus of numerous investigations of their structures and properties [1–12]. Typically, these oxides adopt the orthorhombic $GdFeO_3$ structure type [13], which is a distorted variant of the cubic ABO_3 perovskite structure. Compared with perovskite, in this variant the coordination number of the *A* site is reduced from 12 to 8 and the coordination of the *B* site is reduced from 8 to 6. Magnetic measurements indicate that $LaErO_3$ exhibits an antiferromagnetic transition at 2.4 K [1,12], whereas the $LnYbO_3$ (Ln = La–Pr) compounds order antiferromagnetically with a weak ferromagnetism at 2.7 K [12]. The magnetic properties of these perovskites are independent of the *A* site ions (La–Pr) but are dependent on the *B* site ions (Er and Yb).

In contrast to the oxides, the $LnLn'S_3$ chalcogenides have received little attention and no corresponding selenides $LnLn'Se_3$ or tellurides $LnLn'Te_3$ have been reported. Single-crystal X-ray diffraction studies were conducted on $YScS_3$ [14], $CeScS_3$ [15,16], $CeTmS_3$ [17], $NdYbS_3$ [18], and $LaYbS_3$ [19], but no physical properties were measured. $YScS_3$ and $CeScS_3$ are isostructural and as the $LnLn'O_3$ oxides adopt the $GdFeO_3$ structure type. $CeTmS_3$ crystallizes in a rather complex three-dimensional structure. $LaYbS_3$ crystallizes in two different structure types: α-$LaYbS_3$ (*Pnma*), synthesized at 1520 K, adopts a three-dimensional structure; β-$LaYbS_3$ ($B22_12$; standard setting $C222_1$), synthesized at 1270 K, adopts a layered structure.

This investigation details the syntheses, structure, and magnetic properties of several $LnYbSe_3$ compounds. It also provides a redetermination of the structure of β-$LaYbS_3$, which crystallizes in a different space group from that reported earlier.

2. Experimental

2.1. Syntheses

The following reagents were used as obtained: La (Cerac, 99.9%), Ce (Alfa Aesar, 99.9%), Pr (Strem, 99.9%), Nd (Cerac, 99.9%), Sm (Alfa Aesar, 99.9%), Yb (Strem, 99.9%), S (Alfa Aesar, 99.99%), Se (Cerac,

*Corresponding author. Fax: +1-847-491-2976.
E-mail address: ibers@chem.northwestern.edu (J.A. Ibers).

0022-4596/$ - see front matter © 2003 Elsevier Inc. All rights reserved.
doi:10.1016/j.jssc.2003.08.024

99.99%), and KI (Aldrich, 99.99%). Reaction mixtures consisted of 0.5 mmol *Ln*, 0.5 mmol Yb, and 1.5 mmol S or Se and 300 mg of KI. The reactants were loaded into carbon-coated fused-silica tubes in an Ar filled glovebox. These tubes were sealed under a 10^{-4} Torr atmosphere and then placed in a computer-controlled furnace. The samples were heated to 1223 K in 24 h, kept at 1223 K for 96 h, cooled to 823 K in 144 h, and then rapidly cooled to 295 K. The reaction mixtures were washed with water and dried with acetone. Semiquantitative EDX analyses performed with a Hitachi 3500N SEM confirmed the presence of *Ln*, Yb, and S or Se in a 1:1:3 ratio, in agreement with the final formulation based on the X-ray structure determination. β-$LaYbS_3$ was obtained as yellow needles in less than 10% yield, whereas the *Ln*$YbSe_3$ compounds were obtained as black needles in approximately 50% yield.

2.2. Crystallography

Single-crystal X-ray diffraction data were collected with the use of graphite-monochromatized Mo$K\alpha$ radiation ($\lambda = 0.71073$ Å) at 153 K on a Bruker Smart-1000 CCD diffractometer [20]. The crystal–to–detector distance was 5.023 cm. Crystal decay was monitored by recollecting 50 initial frames at the end of data collection. Data were collected by a scan of 0.3° in ω in groups of 606, 606, 606, and 606 frames at φ settings of 0°, 90°, 180°, and 270°. The exposure times varied from 10 to 20 s/frame. The collection of the intensity data was carried out with the program SMART [20]. Cell refinement and data reduction were carried out with the use of the program SAINT [20] and face-indexed absorption corrections were performed numerically with the use of the program XPREP [21]. Then the program SADABS [20] was employed to make incident beam and decay corrections.

The structures were solved with the direct methods program SHELXS and refined with the full-matrix least-squares program SHELXL of the SHELXTL suite of programs [21]. Each final refinement included anisotropic displacement parameters and a secondary extinction correction. Additional experimental details are given in Table 1. The program STRUCTURE TIDY [22] was used to standardize the positional parameters. The structure of β-$LaYbS_3$ [19] was determined earlier in space group $B22_12$ (standard setting $C222_1$) of the orthorhombic system, although the resultant structure differs minimally from one in *Bbmm* (standard setting *Cmcm*). In space group *Cmcm* there is the systematic absence $h\,0\,l$, $l = 2n$; all other systematic absences are the same in space groups *Cmcm* and $C222_1$. The present data for β-$LaYbS_3$ conform strictly to the condition $h\,0\,l$, $l = 2n$; the structure has been satisfactorily refined in space group *Cmcm*. Fractional coordinates for the six structures determined are listed in Table 2. Selected interatomic distances are given in Table 3.

2.3. Magnetic properties

Magnetic susceptibility measurements on $CeYbSe_3$ (21.5 mg) and $SmYbSe_3$ (31.1 mg) were carried out with the use of a Quantum Design SQUID magnetometer (MPMS5 Quantum Design). The composition of each sample was verified by EDX measurements. The samples were loaded into gelatin capsules. Zero-field cooled (ZFC) susceptibility data were collected in the range 5–300 K. The applied field was 500 G for $CeYbSe_3$ and 200 G for $SmYbSe_3$. All measurements were corrected for core diamagnetism [23]. The susceptibility data in the temperature range 200–300 K were fit by a

Table 1
Crystal data and structure refinements for *Ln*YbQ_3[a]

	Compound					
	β-$LaYbS_3$	$LaYbSe_3$	$CeYbSe_3$	$PrYbSe_3$	$NdYbSe_3$	$SmYbSe_3$
Formula weight	408.13	548.83	550.04	550.83	554.16	560.27
a (Å)	3.9238(8)	4.0616(8)	4.0234(5)	4.0152(5)	4.0015(6)	3.9780(9)
b (Å)	12.632(3)	13.094(3)	13.065(2)	13.053(2)	13.047(2)	13.040(3)
c (Å)	9.514(2)	9.932(2)	9.885(1)	9.868(1)	9.859(1)	9.860(2)
V (Å^3)	471.6(2)	528.2(2)	519.6(1)	517.2(1)	514.7(1)	511.4(2)
ρ_c (g/cm^3)	5.748	6.901	7.031	7.075	7.151	7.276
μ (cm^{-1})	297.68	460.65	473.68	482.09	490.59	507.04
Transm factors	0.23–0.57	0.020–0.16	0.048–0.42	0.074–0.67	0.041–0.36	0.010–0.63
R_1[b]	0.0216	0.0245	0.0177	0.0220	0.0191	0.0235
wR_2[c]	0.0551	0.0562	0.0526	0.0631	0.0526	0.0577

[a] For all structures $Z = 4$, space group = *Cmcm*, $T = 153(2)$ K, and $\lambda = 0.71073$ Å.
[b] $R(F) = \sum||F_o|-|F_c||/\sum|F_o|$ for $F_o^2 > 2\sigma(F_o^2)$.
[c] $R_w(F^2) = \{\sum[w(F_o^2-F_c^2)^2]/\sum wF_o^4\}^{1/2}$ for all data. $w^{-1} = \sigma^2(F_o^2) + (q \times F_o^2)^2$ for $F_o^2 \geq 0$ and $w^{-1} = \sigma^2(F_o^2)$ for $F_o^2 < 0$. $q = 0.03$ for both La compounds; $q = 0.04$ for the others.

least-squares method to the Curie–Weiss equation $\chi = C/(T-\theta_p)$, where C is the Curie constant and θ_p is the Weiss constant. The effective magnetic moment (μ_{eff}) was calculated from the equation $\mu_{eff} = (7.997C)^{1/2}\ \mu_B$ [24].

Table 2
Atomic coordinates[a] and equivalent isotropic displacement parameters for $LnYbQ_3$

Atom	y	z	U_{eq}[b] (Å^2)
β-$LaYbS_3$			
La	0.74651(6)	1/4	0.0049(3)
Yb	0	0	0.0053(3)
S(1)	0.3585(2)	0.0611(3)	0.0066(6)
S(2)	0.0835(3)	1/4	0.0074(9)
$LaYbSe_3$			
La	0.74759(6)	1/4	0.0073(2)
Yb	0	0	0.0073(2)
Se(1)	0.35719(7)	0.0607(1)	0.0074(3)
Se(2)	0.0831(1)	1/4	0.0080(3)
$CeYbSe_3$			
Ce	0.74821(3)	1/4	0.0060(2)
Yb	0	0	0.0064(2)
Se(1)	0.35619(4)	0.06245(5)	0.0070(2)
Se(2)	0.08601(6)	1/4	0.0084(2)
$PrYbSe_3$			
Pr	0.74829(4)	1/4	0.0072(2)
Yb	0	0	0.0068(2)
Se(1)	0.35599(5)	0.06264(7)	0.0073(2)
Se(2)	0.08671(7)	1/4	0.0076(3)
$NdYbSe_3$			
Nd	0.74853(3)	1/4	0.0074(2)
Yb	0	0	0.0071(2)
Se(1)	0.35551(4)	0.06340(5)	0.0074(2)
Se(2)	0.08800(5)	1/4	0.0081(2)
$SmYbSe_3$			
Sm	0.74940(3)	1/4	0.0076(2)
Yb	0	0	0.0075(2)
Se(1)	0.35482(5)	0.06519(7)	0.0081(2)
Se(2)	0.09061(7)	1/4	0.0084(2)

[a] $x = 0$ for all atoms.
[b] U_{eq} is defined as one-third of the trace of the orthogonalized U_{ij} tensor.

3. Results and discussion

3.1. Structure

The $LnYbQ_3$ compounds β-$LaYbS_3$, $LaYbSe_3$, $CeYbSe_3$, $PrYbSe_3$, $NdYbSe_3$, and $SmYbSe_3$ are isostructural to $UFeS_3$ [25]. A view of the unit cell is depicted in Fig. 1. It consists of layers of YbQ_6 (Q = S or Se) octahedra that alternate with layers of LnQ_8 bicapped trigonal prisms along the b-axis. As shown in Fig. 2, the YbQ_6 octahedra share edges along the a-axis and corners along the c-axis to form an infinite buckled sheet. The LnQ_8 bicapped trigonal prisms share edges and caps to form a spacer layer that separates the sheets of YbQ_6 octahedra. The LnQ_8 and YbQ_6 layers are bound together via edge- and corner-sharing of the rare-earth polyhedra to form the overall structure. This structure of the $LnYbQ_3$ materials is closely related to that of the $GdFeO_3$ structure-type adopted by $LnLn'O_3$

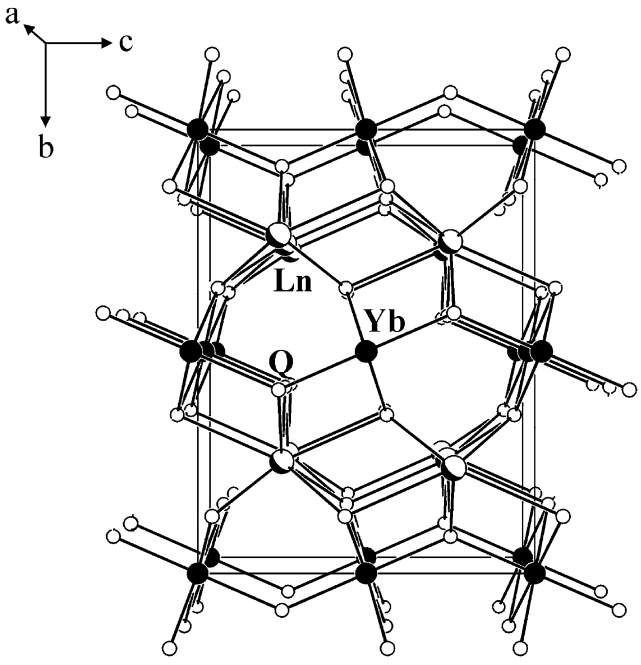

Fig. 1. Unit cell of $LnYbQ_3$ viewed down the a-axis.

Table 3
Selected distances (Å) for $LnYbQ_3$

	Compound					
	β-$LaYbS_3$	$LaYbSe_3$	$CeYbSe_3$	$PrYbSe_3$	$NdYbSe_3$	$SmYbSe_3$
Ln–$Q(1)\times 4$	3.013(2)	3.1173(9)	3.0780(5)	3.0700(6)	3.0555(5)	3.0275(7)
Ln–$Q(1)\times 2$	3.244(3)	3.377(1)	3.3763(7)	3.3720(8)	3.3749(7)	3.392(1)
Ln–$Q(2)\times 2$	2.844(3)	2.960(1)	2.9218(7)	2.9117(8)	2.8965(6)	2.8712(9)
Yb–$Q(1)\times 4$	2.717(2)	2.8258(8)	2.8210(4)	2.8189(5)	2.8191(4)	2.8201(6)
Yb–$Q(2)\times 2$	2.602(2)	2.7109(7)	2.7147(4)	2.7142(5)	2.7190(4)	2.7334(7)
$Ln\cdots$Yb	3.9889(9)	4.1338(9)	4.1143(5)	4.1086(5)	4.1036(5)	4.0931(8)

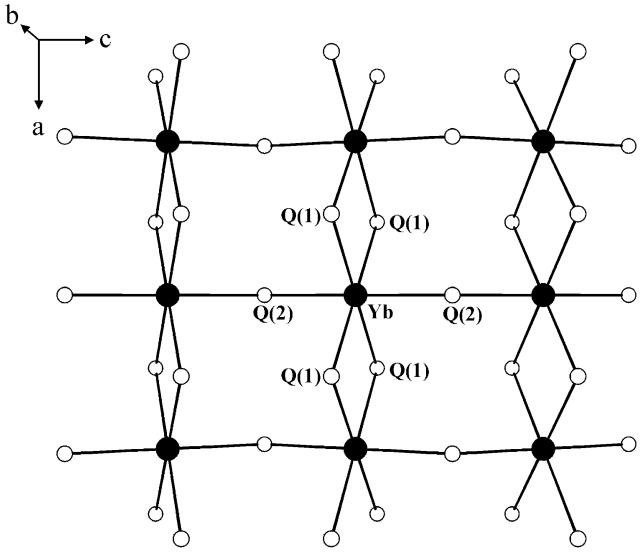

Fig. 2. YbQ_6 layer viewed down the *b*-axis.

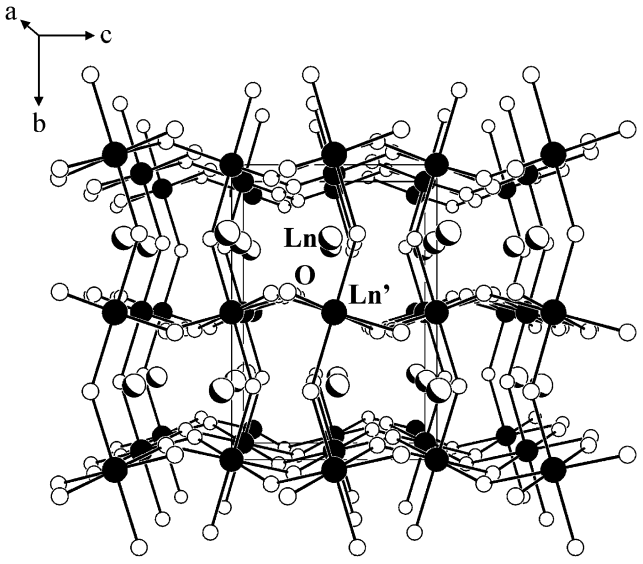

Fig. 3. Unit cell of the $GdFeO_3$-type $LnLn'O_3$ compounds viewed down the *a*-axis. The *Ln*–O bonds have been removed for clarity.

(*Ln* = La–Nd; *Ln*′ = Ho–Lu, Y) and $LnScS_3$ (*Ln* = Ce, Y) (space group *Pnma*) [13]. The distorted perovskite phase, pictured in Fig. 3, is constructed from $Ln'O_6$ octahedra that share edges and corners along the *a* and *c*-axis to form a buckled sheet similar to that of the YbQ_6 octahedra in $LnYbQ_3$. However, the $Ln'O_6$ octahedra of the perovskite compounds participate in additional corner-sharing along the *b*-axis to form a three-dimensional tunnel structure. The *Ln* atoms reside within these tunnels and are coordinated to eight O atoms in a bicapped trigonal prismatic arrangement.

The structure of β-$LaYbS_3$ found here differs minimally from that reported earlier [19], although the

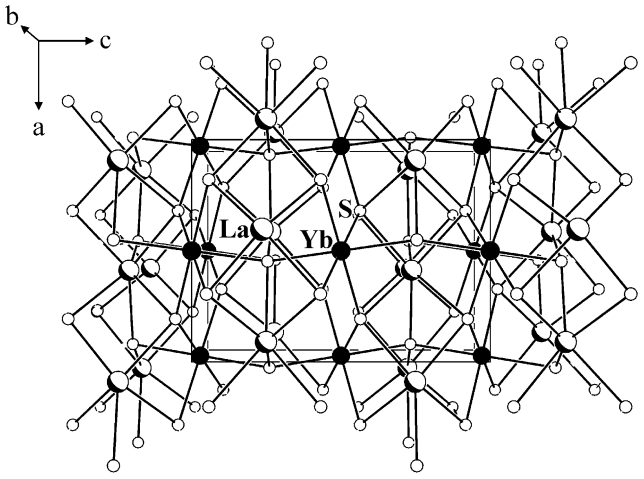

Fig. 4. Structure of α-$LaYbS_3$.

present results suggest that the earlier determinations of the structures of both β-$LaYbS_3$ and $NdYbS_3$ [18] were carried out in the wrong space group, as was the case for $CeScS_3$ [15,16]. In contrast, the structure of α-$LaYbS_3$ [19], Fig. 4, is significantly different from that of the other materials. This complex three-dimensional structure is composed of distorted LaS_6 trigonal prisms and YbS_6 octahedra and bears little resemblance to the layered structures described here.

In the $LnYbQ_3$ materials all of the bond lengths are normal (Table 3). The following comparisons can be made: La–S, 2.844(3)–3.244(3) vs. 2.89(1)–3.14(2) Å in $La_2Fe_2S_5$ [26]; La–Se, 2.960(1)–3.377(1) vs. 2.975(3)–3.222(5) Å in $La_3AgSiSe_7$ [27]; Ce–Se, 2.9218(7)–3.3763(7) vs. 3.0027(9)–3.0253(9) Å in KCe_2CuSe_6 [28]; Pr–Se, 2.9117(8)–3.3720(8) vs. 2.970(2)–3.281(2) Å in Pr_3InSe_6 [29]; Nd–Se, 2.8965(6)–3.3749(7) vs. 2.970(1)–3.152(2) Å in $NdSe_{1.9}$ [30]; Sm–Se, 2.8712(9)–3.392(1) vs. 2.9285(8)–3.296(1) Å in Sm_3CrSe_6 [31]; Yb–S, 2.602(2)–2.717(2) vs. 2.677(2)–2.694(2) Å in $CaYbInS_4$ [32]; and Yb–Se, 2.7109(7)–2.8258(8) vs. 2.804(2)–2.818(2) Å in $CaYbInSe_4$ [32]. Because there are no *Q*–*Q* bonds in the structure of $LnYbQ_3$ the formal oxidation states of *Ln*/Yb/*Q* are 3+/3+/2−.

3.2. Magnetic properties

$CeYbSe_3$ and $SmYbSe_3$ are paramagnetic in the range 5–300 K (Fig. 5). Both compounds deviate from ideal Curie–Weiss behavior at low temperatures (< 100 K) as a result of crystal-field effects [33]. The values of *C* (emu K mol^{-1}), θ_p (K), and μ_{eff} (μ_B) for the materials are: $CeYbSe_3$, 3.46(7), −44.6(9), 5.26(6); $SmYbSe_3$, 2.11(8), −107.6(4), 4.11(7). The large negative values of θ_p are indicative of a substantial degree of local antiferromagnetic coupling and it is possible that these materials order antiferromagnetically below 5 K, as do the $LnLn'O_3$ materials. The values of μ_{eff} agree well with

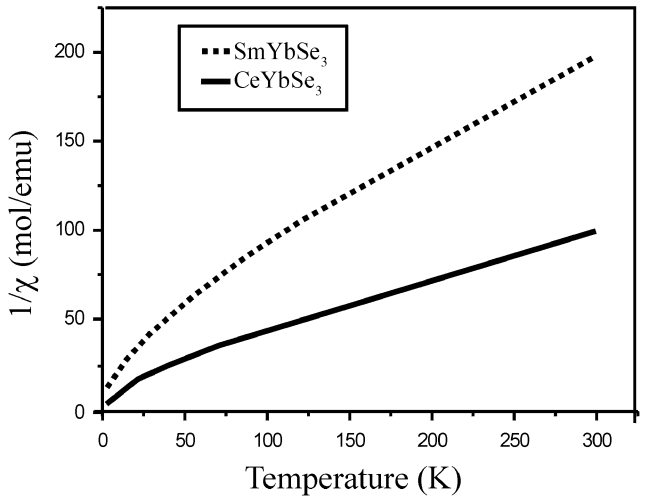

Fig. 5. Inverse magnetic susceptibility ($1/\chi$) vs. T for $CeYbSe_3$ and $SmYbSe_3$.

the theoretical values of 5.20 and 4.78μ_B, calculated for $CeYbSe_3$ and $SmYbSe_3$ from the magnetic moments for Ce^{3+}, Sm^{3+}, and Yb^{3+} of 2.54, 1.5, and 4.54 μ_B, respectively [34].

Acknowledgments

This research was supported by National Science Foundation Grant DMR00-96676 and a Ford Predoctoral Fellowship to K.M. Use was made of the Central Facilities supported by the MRSEC program of the National Science Foundation (DMR00-76097) at the Materials Research Center of Northwestern University.

References

[1] J.M. Moreau, J. Mareschal, E.F. Bertaut, Solid State Commun. 6 (1968) 751–756.
[2] H. Müller-Buschbaum, C. Teske, Inorg. Nucl. Chem. Lett. 4 (1968) 151–152.
[3] J.M. Moreau, Mater. Res. Bull. 3 (1968) 427–432.
[4] J. Mareschal, J.M. Moreau, G. Ollivier, P. Pataud, J. Sivardiere, Solid State Commun. 7 (1969) 1669–1672.
[5] H. Müller-Buschbaum, C. Teske, Z. Anorg. Allg. Chem. 369 (1969) 255–264.
[6] H. Müller-Buschbaum, P.-H. Graebner, Z. Anorg. Allg. Chem. 386 (1971) 158–162.
[7] U. Berndt, D. Maier, C. Keller, J. Solid State Chem. 13 (1975) 131–135.
[8] J. Coutures, J.P. Coutures, J. Solid State Chem. 19 (1976) 29–33.
[9] U. Berndt, D. Maier, C. Keller, J. Solid State Chem. 16 (1976) 189–195.
[10] M. Deepa, U.V. Varadaraju, Mater. Res. Soc. Symp. Proc. 527 (1998) 507–511.
[11] M. Itoh, K. Tezuka, M. Wakeshima, Y. Hinatsu, J. Solid State Chem. 145 (1999) 104–109.
[12] K. Ito, K. Tezuka, Y. Hinatsu, J. Solid State Chem. 157 (2001) 173–179.
[13] M. Marezio, J.P. Remeika, P.D. Dernier, Acta Crystallogr. Sect. B: Struct. Crystallogr. Cryst. Chem. 26 (1970) 2008–2022.
[14] N. Rodier, P. Laruelle, C. R. Seances Acad. Sci. Ser. C 270 (1970) 2127–2130.
[15] D.J.W. Ijdo, Acta Crystallogr. Sect. B: Struct. Crystallogr. Cryst. Chem. 36 (1980) 2403–2404.
[16] K.-J. Range, A. Gietl, U. Klement, Z. Kristallogr. 207 (1993) 147–148.
[17] N. Rodier, Bull. Soc. Fr. Mineral. Cristallogr. 96 (1973) 350–355.
[18] D. Carré, P. Laruelle, Acta Crystallogr. Sect. B: Struct. Crystallogr. Cryst. Chem. 30 (1974) 952–954.
[19] N. Rodier, R. Julien, V. Tien, Acta Crystallogr. Sect. C: Cryst. Struct. Commun. 39 (1983) 670–673.
[20] Bruker, SMART Version 5.054 Data Collection and SAINT-Plus Version 6.22 Data Processing Software for the SMART System, 2000 (Bruker Analytical X-ray Instruments, Inc., Madison, WI, USA).
[21] G.M. Sheldrick, SHELXTL DOS/Windows/NT Version 6.12, 2000 (Bruker Analytical X-ray Instruments, Inc., Madison, WI, USA).
[22] L.M. Gelato, E. Parthé, J. Appl. Crystallogr. 20 (1987) 139–143.
[23] L.N. Mulay, E.A. Boudreaux, Theory and Applications of Molecular Diamagnetism, Wiley-Interscience, New York, 1976.
[24] C.J. O'Connor, Prog. Inorg. Chem. 29 (1982) 203–283.
[25] H. Noël, J. Padiou, Acta Crystallogr. Sect. B: Struct. Crystallogr. Cryst. Chem. 32 (1976) 1593–1595.
[26] F. Besrest, G. Collin, J. Solid State Chem. 21 (1977) 161–170.
[27] S.-H. Lin, J.-G. Mao, G.-C. Guo, J.-S. Huang, J. Alloys Compd. 252 (1997) L8–L11.
[28] Y. Klawitter, C. Näther, I. Jess, W. Bensch, M.G. Kanatzidis, Solid State Sci. 1 (1999) 421–431.
[29] L.E. Aleandri, J.A. Ibers, J. Solid State Chem. 79 (1989) 107–111.
[30] W. Urland, P. Plambeck-Fischer, M. Grupe, Z. Naturforsch. B: Chem. Sci. 44 (1989) 261–264.
[31] O. Tougait, J.A. Ibers, Inorg. Chem. 39 (2000) 1790–1794.
[32] J.D. Carpenter, S.-J. Hwu, Chem. Mater. 4 (1992) 1368–1372.
[33] C. Cascales, R. Sáez-Puche, P. Porcher, J. Solid State Chem. 114 (1995) 52–56.
[34] C. Kittel, Introduction to Solid State Physics, 6th Edition, Wiley, New York, 1986.